

1 Supplementary information

2 Contents

3	1	Test criteria for method development.....	3
4	1.1	Recovery calculation.....	3
5	1.1.1	Si bulk mass recovery ($rec_{Si,bulk}$).....	3
6	1.1.2	AF ⁴ recovery (rec_{AF4}).....	3
7	1.1.3	Total Si mass recovery ($rec_{Si,total}$).....	4
8	1.2	Particle size distribution calculation.....	4
9	1.2.1	Approach 1 based on MALS:.....	4
10	1.2.2	Approach 2 based on AF ⁴ calibration:.....	5
11	2	Methodology for the separation of SiO ₂ nanoparticles.....	5
12	2.1	Sample homogenization (step I).....	5
13	2.2	Acid digestion of tomato soup matrix (step II.1).....	6
14	2.3	Colloidal extraction (step II.2).....	7
15	2.4	Particle concentration enrichment (step III).....	8
16	2.5	Stabilisation of the particles (step IV).....	8
17	3	Characterization of the pure SiO ₂ -ENP suspension.....	9
18	3.1	Recovery.....	9
19	3.2	Particle size distributions.....	9
20	4	Acid digestion for extraction of SiO ₂ -ENPs from tomato soup.....	11
21	4.1	Recovery.....	11
22	4.2	Particle morphology.....	12
23	4.3	Particle distribution after sonication (step IV).....	12
24	5	Colloidal extraction of SiO ₂ -ENPs from tomato soup.....	13
25	5.1	Colloidal extraction: Si mass recovery.....	13
26	5.2	Colloidal extraction: particle size distribution.....	14

27	6	Signal intensities during ICP-MS analysis of SiO ₂ -ENPs	14
28	7	Stability of SiO ₂ -ENP suspension.....	15
29	8	References.....	15
30			
31			

32 **1 Test criteria for method development**

33 **1.1 Recovery calculation**

34 Three different recoveries were defined: Si bulk mass recovery, sample recovery following AF⁴
35 separation, and total Si recovery.

36 1.1.1 Si bulk mass recovery ($\text{rec}_{\text{Si,bulk}}$)

37 The Si bulk mass recovery ($\text{rec}_{\text{Si,bulk}}$) is defined as

$$38 \quad \text{rec}_{\text{Si,bulk}} = c_{\text{Si,sample,ICP-OES}} / c_{\text{Si,initial}} \cdot 100 \quad [\%] \quad (\text{Equation 1})$$

39 where ($c_{\text{Si,sample,ICP-OES}}$) is the Si mass concentration after the sample preparation procedure, as
40 determined by ICP-OES analysis, and ($c_{\text{Si,initial}}$) is the initial Si mass concentration, calculated from the
41 SiO₂ mass concentration in the stock solutions and converted into SiO₂ concentration of the respective
42 sample (compare Table 1 of main the text).

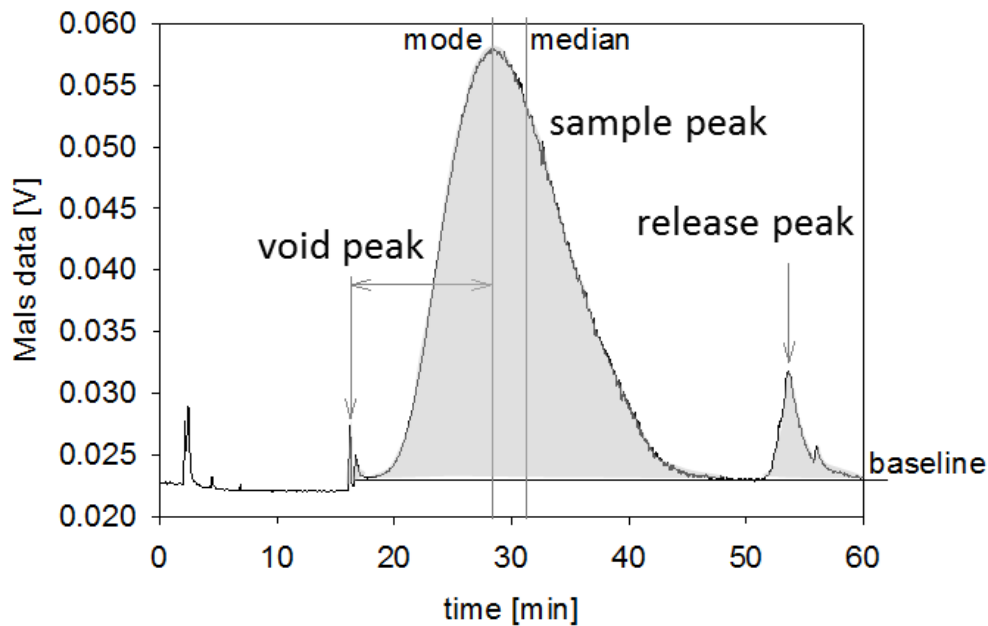
43 1.1.2 AF⁴ recovery (rec_{AF4})

44 The AF⁴ recovery (rec_{AF4}) is based on the MALS data acquired during AF⁴ analysis. Assuming that no
45 significant quantities of particles other than SiO₂-ENPs are present in the suspension, the MALS signal
46 can be considered to be semi-quantitative. The AF⁴ recovery after separation in the AF⁴ system is
47 defined as:

$$48 \quad \text{rec}_{\text{AF4}} = A_{\text{FFF,sample}} / A_{\text{Rec,sample}} \cdot 100 \quad [\%] \quad (\text{Equation 2})$$

49 where ($A_{\text{FFF,sample}}$) is the area under the peak for an AF⁴ run with field force (i.e. cross flow) and
50 ($A_{\text{Rec,sample}}$) is the area under the peak for an AF⁴ run without field force.

51 There were usually three peaks in the fractogram following AF⁴-separation, the void peak, the sample
52 peak, and the release peak (Figure A-1). The void peak was due to unretained particles and the release
53 peak to particles temporarily attached to the membrane. The sample peak represents the fractionated
54 particles. All three peaks were used for the recovery calculations.



55

56 Figure A-1: AF⁴-fractogram monitored with the MALS signal

57

58 Since AF⁴-recovery is only semi-quantitative carry-over of particulate material introduces the risk that
 59 the SiO₂-ENP recovery might be overestimated due to the false detection of particles by MALS, which
 60 are not SiO₂-ENPs.

61 1.1.3 Total Si mass recovery ($rec_{Si,total}$)

62 Total Si mass recovery ($rec_{Si,total}$) after size separation is determined by:

$$63 \quad rec_{Si,total} = n_{Si,sample,ICP-MS} / n_{Si,initial} \cdot 100 \quad [\%] \quad (\text{Equation 3})$$

64 where $n_{Si,sample,ICP-MS}$ is the total Si mass content following size separation, as determined by Si mass
 65 quantification using ICP-MS coupled online to the AF⁴-system, and ($n_{Si,initial}$) is the known initial Si
 66 mass content.

67 1.2 Particle size distribution calculation

68 1.2.1 Approach 1 based on MALS:

69 ASTRA Software (Version 5) provides eight different models (Zimm, Debye, Berry, Random Coil,
 70 Sphere, Coated Sphere, Rod, and Mie) for calculating the radii of particles from the MALS data.
 71 Additionally, it allows the user to select between various fitting orders such as Debye 3rd order. The

72 quality of size fitting for spherical particles (Nanosphere™ particle size standards) in the size range of
73 the analysed SiO₂-ENPs decreases in the following order: Sphere > Debye 3rd >> Berry > Zimm ¹. For
74 heterogeneously shaped (essentially non-spherical) particles the quality of the size fitting decreases in
75 the following order: Zimm > Debye >> Sphere & Berry. All models were tested and one particular
76 model selected on the basis of the available information on particle shape, and on a comparison of the
77 model results with size data (hydrodynamic radius) derived from the second approach. We decided to
78 use the Debye 3rd order model to calculate the size distributions from the MALS data because of its
79 robustness and fitting capabilities for both spherical and non-spherical particles ¹. The Debye model
80 also provides the radius of gyration, which is otherwise known as the root mean square radius (r_{rms}).
81 The r_{rms} , (as defined in von der Kammer *et al.*¹) takes into account the mass distribution within the
82 particle and is hence shape sensitive ¹.
83 The size distribution function obtained by MALS is intensity weighted. However, since the MALS
84 measurement is done after the particle size fractionation in the AF⁴ small particles are still detectable.

85 1.2.2 Approach 2 based on AF⁴ calibration:

86 The r_h size distribution was determined after AF⁴-calibration with polystyrene standards (PS standards
87 with diameters of 50, 100, and 150 nm: Thermo Scientific). A linear size calibration method employed
88 resembled the typical $\lambda = 6 \cdot R$ linear approximation (R retention factor) in FFF theory and follows the
89 equation: $t_R = 0.0856 r_h + 0.0578$ with $R^2=0.999$.

90

91 **2 Methodology for the separation of SiO₂ nanoparticles**

92 **2.1 Sample homogenization (step I)**

93 Three different techniques were tested for homogenization of the tomato soup samples (either as
94 stand-alone techniques or in combination):

95 (1) manual agitation: The sample was shaken by hand for 15 seconds. Fat and organic fiber material
96 were dispersed and suspended in the aqueous solution.

97 (2) heating: The sample was heated at 50°C in a water bath for 30 minutes, during which time fatty
98 constituents of the tomato soup were dispersed and dissolved.

99 (3) mechanical mixing: An IKA T10 basic Ultra Turrax stainless steel dispersing instrument was
100 operated for 30 seconds at 20,000 - 25,000 rpm, broke down most of the organic fiber material and
101 dispersed the fat.

102 Following each of the tests an aliquot of 1.5 g was removed from the stock suspension using a
103 stainless steel sampling spoon.

104 **2.2 Acid digestion of tomato soup matrix (step II.1)**

105 Two different procedures were tested for acid digestion in order to optimize the energy input. The two
106 types of acid digestion were performed with the samples SiO₂-ENP, TS+SiO₂-ENP, and TS+SiO₂-
107 ENP_{aged}. Additional blank MQ-water and tomato soup samples were run for quality control. The initial
108 SiO₂-ENP and organic matter concentrations were similar in all samples.

109 1) Heating and bath sonication. 2 mL of tomato soup, 0.5 mL of SiO₂-ENP, and 7.5 mL of MQ-water
110 were first well mixed. The SiO₂ mass concentration in the mixture was 2 g_{SiO₂} L⁻¹. Blanks were
111 prepared with 2 mL of pure tomato soup and 8 mL of MQ-water. 2 mL of this solution were added to
112 8 mL of HNO₃ (65% Merck, Suprapure®) and 2 mL of H₂O₂ (30% Merck super pure), to make a total
113 volume of 12 mL. The prepared suspension was then sonicated for 30 minutes at 90°C. Following
114 temperature adjustment to 25°C the sample was diluted with MQ-water by a factor of 1:10. The
115 sample was further diluted with MQ-water in two steps (1:50 and 1:100) to achieve 1:5,000 dilution
116 for ICP-MS [analysis](#).

117 2) Microwave-assisted digestion. 2 mL of the sample were first poured into the Teflon® digestion
118 tubes. In order to oxidize the organic carbon matrix, 1 mL H₂O₂ (30%; Merck supra pure) and 5 mL
119 HNO₃ (65%; Merck supra pure) were added prior to microwave assisted digestion (Microwave 3000,
120 Anton Paar, USA), which results in an increase in pressure and temperature. Samples were heated
121 stepwise for 27 minutes (0-5 min: 0-250 W; 5-7 min: 250 W; 7-12 min: 250-750 W; 12-27 min: 750
122 W; cooling: 27-42 min: 0 W), achieving a maximum temperature of 200°C. The pressure maximum in
123 each digestion tube was set to 60 bar. After cooling down, the acidic samples were transferred from

124 the digestion tubes to volumetric flasks and filled to 100 mL using MQ-water, introducing a 1:50
125 sample dilution. The acidic samples were stored in 100 mL PE bottles.

126 To determine the Si bulk mass recovery the digested samples were tip sonicated for 90 seconds (0.05
127 kJ mL⁻¹, Bandelin Sonoplus, Germany) and 3 mL then diluted 1:10 with FFF carrier solution (0.025%
128 (v/v) FL-70™). The diluted samples were then immediately analyzed for Si content by ICP-OES.

129 **2.3 Colloidal extraction (step II.2)**

130 During colloidal extraction the separation of particles from the matrix was attempted by the addition
131 of extractants to obtain individual ENPs, by dilution, and using mechanical energy input to destroy
132 aggregates of SiO₂-ENPs and matrix components (fat, fibers). The all type of colloidal extractions
133 were performed with the samples SiO₂-ENP, TS+SiO₂-ENP, and TS+SiO₂-ENP_{aged}. Each of the
134 extraction agents was adjusted to a pH of 9 prior to the experiments. Indeed, SiO₂-ENP suspensions
135 show improved colloidal stability in slightly alkaline conditions, the pH was adjusted to 9 when
136 necessary, using NaOH. The ENP-surfaces are then negatively charged (PZC = 2;² zeta potential
137 (pH=9) < -30 mV) and aggregation of SiO₂-ENPs is less likely to occur. However, the ionic strength
138 of the extractants was not matched.

139 For all colloidal extraction 1.5 g of samples (TS+SiO₂-ENP or TS+SiO₂-ENP_{aged}) were mixed with
140 13.5 mL of extractants. 3 types of extracting agent were used:

141 MQ-water was used for baseline testing to determine the individual effects of dilution and mechanical
142 energy input.

143 Ammonium carbonate (0.25, 2.5, and 25 mmol L⁻¹). Ammonium carbonate (AC) was selected as a
144 buffer because of its compatibility with later ICP-MS analysis. High AC concentrations (c(AC)=25
145 mmol L⁻¹ and IS = 75 mmol L⁻¹) are likely to destabilize any other particles in the suspension because
146 of the ionic strength. SiO₂-ENPs were, however, stable under these conditions as indicated by
147 preliminary tests (Table A-2).

148 FL-70™ solution (0.025, and 0.05% (v/v)). The FL-70™ solution, as a mixture of a variety of
149 surfactants (ionic and anionic), has the potential to stabilize particles with heterogeneously charged
150 surfaces. Besides, FL70 has shown stabilizing properties during FFF separations.

151 In addition to the type of extraction agent used, the mechanical energy input and agitation time were
152 also tested for their effects on Si mass recovery and method duration. In order to accelerate SiO₂-ENP
153 extraction mechanical energy was provided either by agitation or by sonication. To determine the
154 minimum extraction time required for maximum recovery the mixture was agitated for 0.5, 1, 3, 5, 8,
155 16, 24, and 72 hours at 200 rpm on a horizontal shaker. The mixture was then centrifuged for 30
156 minutes at 1,700 rpm (cut off equals 400 nm, Jouan CR422, Thermo Scientific, USA) and the Si
157 content of the supernatant analyzed using ICP-OES. Particle characterization was performed using
158 DLS and AF⁴-MALS. Particulate matter content was further quantified by UV absorbance
159 measurements at 280 nm (UV/vis Spectrometer, Lambda 35, Perkin Elmer).

160 ***2.4 Particle concentration enrichment (step III)***

161 Particle concentration enrichment (III) and particle stabilization (IV) were carried out immediately
162 after microwave digestion. Subsamples (each of 20 mL) of acid digested solutions were centrifuged at
163 4,500 rpm for 15 minutes (Jouan CR 422, USA) in order to enrich the ENP concentration. After
164 centrifugation a 10 mL volume of the supernatant was analyzed by ICP-OES in order to determine the
165 mass of Si which was not concentrated during centrifugation. From this measurement the Si mass in
166 the remaining liquid (i.e. concentrate) was found to have increased by a factor of approximately 2.4.
167 The ENP concentration in the colloidal extract (II.2) was not enriched.

168 ***2.5 Stabilisation of the particles (step IV)***

169 The objective of the ENP stabilization was twofold: (a) to break up any aggregates that had formed
170 during the separation, and (b) to prevent re-aggregation during further analysis. The colloidal
171 extraction required no further particle stabilization as the pH and ionic strength in the extract did not
172 promote particle aggregation or dissolution. However, acid digestion introduced marked changes in
173 the hydrochemical conditions (pH, ionic strength). Indeed, the point of zero charge (PZC) of SiO₂-
174 ENPs (between 2.2 and 3.4²) was crossed during acid digestion, aggregation of the particles was
175 likely. Therefore, the particle suspensions needed to be stabilized by re-adjusting the pH and ionic
176 strength in order to avoid particle aggregation or dissolution. Adjustment of the ionic strength was

177 achieved through the use of a dilution/extraction agent (e.g. salt or detergent solution). In practice the
178 suspension was diluted by the factor of 10 in 0.025% FL-70™ solution. The pH adjustment to values
179 between 7 and 8 was achieved by adding NaOH solution (0.1 or 0.01 mol L⁻¹). After 12 hours the
180 suspensions of the stabilized particles were again characterized.
181 Besides, sonication was used following pH adjustment to break up any possible
182 aggregates/agglomerates. Size distributions after sonication for 0, 45, 90, and 120 seconds were
183 compared with the original size distribution of the undigested reference sample.

184 **3 Characterization of the pure SiO₂-ENP suspension**

185 As a first step the pure particle suspension was characterized in terms particle size distribution and the
186 recovery was calculated for the analytical method. The data were used as a benchmark and compared
187 with the particle size distribution of the extracted SiO₂-ENPs from tomato soup by various sample
188 preparation methods. Additional data on characterization of the pure particle suspension is also
189 provided by Grombe *et al.*³

190 **3.1 Recovery**

191 Following water bath sonication and dilution to approximately 100 mg L⁻¹ the AF⁴ mass recovery
192 (rec_{AF4}) from the pure SiO₂-ENP suspension was 90%. Total Si mass recovery (rec_{Si,total}) was in the
193 same range (97%). The mass loss was attributed to an accumulation of material on the surface of the
194 membrane, which was not released during sample fractionation. Regular system-cleaning runs were
195 therefore performed (by injecting 10 μL of iso-propanol) in order to avoid long-term accumulation of
196 SiO₂-ENPs within the FFF system. Recovery data indicated that the applied AF⁴ size separation
197 worked sufficiently.

198 **3.2 Particle size distributions**

199 The hydrodynamic radius ($r_{h,DLS}$) obtained from the DLS measurements was 68 nm. The r_h -size
200 distribution obtained from the AF⁴-calibration had its maximum at 63 nm, with a standard deviation
201 (s.d.) of 2 nm from the mean value (Figure 2, main manuscript). The median hydrodynamic radius
202 ($r_{h,median}$) derived from AF⁴-calibration of 70 ± 5 nm was larger than the mode and the mode/median

203 ratio was 0.90 ± 0.04 , indicating a tailing of the size distribution. Since the MALS-derived light
204 scattering intensity is used to establish a size distribution from AF⁴ fractograms, the distribution
205 function obtained is intensity weighted. This weighting becomes more pronounced as the detection
206 angle decreases (i.e. particle size increases), and the intensity-weighted size distributions of poly-
207 disperse samples are therefore biased towards larger radii. For particles with a constant, known
208 stoichiometry a true particle mass based size distribution (which is not affected by the particle size)
209 can be derived from the ²⁸Si ICP-MS signal, which was recorded online following size separation
210 using AF⁴. As expected, the Si mass based size distribution (based on the r_h) derived from ICP-MS
211 quantification showed generally smaller particle sizes than the MALS-based size distribution.¹ The
212 median r_h was determined to be 54 nm and the mode 43 nm, resulting in a mode/median ratio of 0.80.
213 The mass-based size distribution approached a lognormal distribution, as depicted in Figure 2 of the
214 main manuscript.

215 Similar SiO₂-ENPs were used to spike the tomato soup. The size distribution of SiO₂-ENPs extracted
216 from the tomato soup is expected to show similar properties. Therefore, the sample preparation was
217 adjusted until both size distributions (from the pure suspension and from particles extracted from the
218 tomato soup) were likewise. In order to identify possible bias of the size distribution due to sample
219 preparation both pure particle suspensions and tomato soup were treated by the respective sample
220 preparation procedure.

221 The r_{rms} based on MALS data increased linearly across most of the size distribution (Figure 2 a, main
222 manuscript). Exceptions were small particles with $r_h < 30$ nm and large particles with $r_h > 100$ nm. The
223 r_{rms} data in the lower range of the size distribution (< 30 nm) was likely influenced by incomplete void
224 peak separation, as indicated by increasing radii towards the void peak. The r_{rms}/r_h ratio, which can be
225 used as an indicator of particle shape, had values between 1.0 and 1.2 indicating an ideal particle size
226 separation, but also indicating that the fumed silica particles are not homogeneous spheres.¹

227

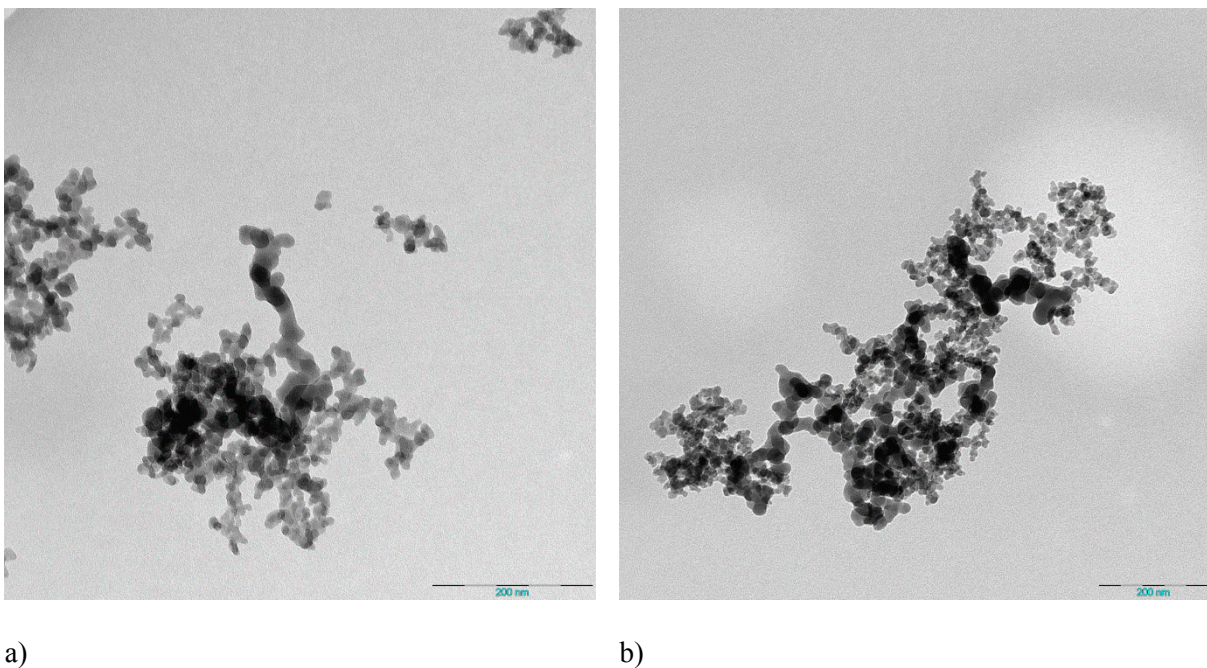
228 4 Acid digestion for extraction of SiO₂-ENPs from tomato soup

229 4.1 Recovery

230 The Si bulk recovery ($\text{rec}_{\text{Si,bulk}}$) was close to 100% for all samples using either sonication + heating or
231 microwave-assisted digestion. However, organic matrix oxidation was more complete with microwave
232 assistance than with sonication and heating, as was indicated by the loss of the yellowish colour in the
233 sample suspension following microwave-assisted digestion. Microwave-assisted acid digestion was
234 therefore used to further optimize sample preparation.

235 4.2 Particle morphology

236 Possible alteration of SiO₂-ENPs, caused acid digestion, were investigated by TEM analysis (CM 100
237 BioTWIN at 80kV). Image analysis did not indicate a change in particle morphology or size of the
238 primary particle size due to acid digestion (Figure A-2).



239 Figure A-2: TEM analysis of a) SiO₂-ENPs and b) SiO₂-ENPs extracted from tomato soup via acid
240 digestion [after tip sonication](#) (90 s), both size bars 200 nm

241 **4.3 Particle distribution after sonication (step IV)**

242 Parameters of the size distribution of SiO₂-ENPs extracted from tomato soup after different times of
243 tip sonication are provided in Table A-1. Indications that the composition of the dilution media had
244 effect on the size distribution (0.025% FL-70TM or 0.25 mmol L⁻¹ AC) were observed. For practical
245 considerations regarding AF⁴ separation 0.025% FL-70TM was selected for use as dilution agent and
246 stabilization agent for separated SiO₂-ENPs.

247

248 Table A-1: Peak evaluation after different sonication times for the pure SiO₂-ENP suspension after
249 acid digestion based on the MALS signal; uncertainty is expressed as standard deviation from the
250 mean value of triplicate analysis

sonication time [s]	stabilization agent [-]	r_h, mode [nm]	r_h, median [nm]	peak shape factor [-]
0	FL-70 TM	137 ± 1	126 ± 1	1.09
45	FL-70 TM	111 ± 1	108 ± 1	1.03
90	FL-70 TM	97 ± 1	101 ± 1	0.96
90	AC	107	126	0.85
135	FL-70 TM	88 ± 1	93 ± 3	0.95
SiO ₂ -ENP <small>(no acid digestion)</small>	FL-70 TM	63 ± 2	70 ± 5	0.90

251

252 **5 Colloidal extraction of SiO₂-ENPs from tomato soup**

253 The objective of Colloidal extraction is separating the SiO₂-ENPs without any destruction or
254 dissolution of the matrix. It is a far gentler and less invasive method that could potentially also be used
255 for more vulnerable particles such as silver-ENPs or copper-ENPs.

256 **5.1 Colloidal extraction: Si mass recovery**

257 The maximum $rec_{Si,bulk}$ was obtained with extraction by 2.5 mmol L⁻¹ AC-solution, but this
258 corresponds to only 12 ± 2% (Table A-2). The extraction efficiency followed the order of (AC) > (FL-
259 70TM) > (MQ-water) (Tab. A-2). The data suggest that none of the extraction agents were able to break

260 the bonds between silica particles and particulate tomato soup matrix within the 30 minute extraction
 261 period.

262 Table A-2: Si mass recovery ($rec_{Si,bulk}$ [%]) after a 30 minute extraction period for tomato soup spiked
 263 with SiO₂-ENPs (both aged and freshly spiked) and for pure SiO₂-ENP suspension, using different
 264 concentrations of ammonium carbonate and FL-70TM. Errors are indicated by single standard
 265 deviations calculated from triplicates

Type of extraction agent and concentration	SiO₂-ENP [%]	TS+SiO₂-ENP [%]	TS+ SiO₂-ENP_{aged} [%]
ammonium carbonate			
(mM)			
0.25	90±9	n/a	2±0
2.5	94±4	90±3	12±2
25	93±5	93±2	7±4
FL-70 (% , v/v)			
0.025	85±4	n/a	1±0.2
0.25	90±3	n/a	5±1
2.5	84±4	n/a	5±3
MQ-water			
	86±3	n/a	1±1

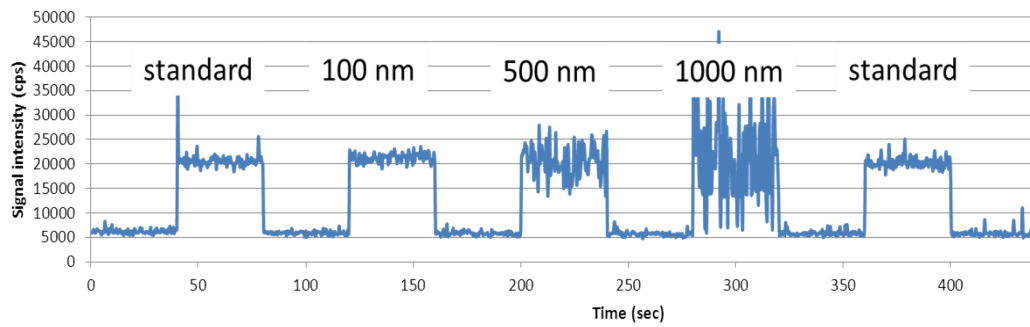
266

267 **5.2 Colloidal extraction: particle size distribution**

268 Following colloidal extraction, particles in the tomato soup extracts showed a six times higher UV-
 269 light absorbance at 280 nm ($abs_{280}=0.59$ mAU) than those in the pure particle suspension
 270 ($abs_{280}=0.09$ mAU), indicating poor separation of the target particles from the matrix and the presence
 271 of matrix residue within the extract. The total particulate matter content after colloidal extraction
 272 followed by centrifugation was too high for further size characterization with FFF-ICP-MS. Filtration
 273 (5 µm, nylon) was therefore used as an additional clean-up step, but this resulted in a significantly
 274 lower Si mass recovery. The Si mass recovery fell from 26% to 20% after filtration, which is
 275 equivalent to a Si mass loss of 21%. Incomplete separation during the sample preparation meant that
 276 particle size and concentration could not be correctly determined by FFF-MALS-ICP-MS.

277 **6 Signal intensities during ICP-MS analysis of SiO₂-ENPs**

278 The response of the mass detector depending on different particle size is depicted in Figure A-3. All
 279 particle sizes were measured at similar concentrations and there was no difference in signal intensity
 280 observed. The signal noise increased with increasing particle size and constant Si concentration which
 281 results in a decreased measurement precision of the ICP-MS.



282

283 Figure A-3: ICP-MS ²⁸Si signal intensities from the dissolved standard and from 100, 500, and
 284 1000 nm SiO₂-ENPs (Postnova analytics), all at similar mass concentrations

285 **7 Stability of SiO₂-ENP suspension**

286 Simovic & Prestidge⁴ reported a critical coagulation concentration for hydrophobic silica (0.25%
 287 (m/m)) of between 10 and 100 mmol L⁻¹ ionic strength at pH values of 7 and 9, respectively.
 288 Preliminary tests with different ionic strength concentrations have confirmed the data shown here
 289 (Table A-3).

290 Table A-3: Hydrodynamic radii determined by DLS of SiO₂-ENPs in suspension (100 mg L⁻¹) at
 291 various ionic strengths (measured as triplicates)

Time:	1 h		3 h		5 h	
c(NaCl)	average	std.dev.	average	std.dev.	average	std.dev.
mmol L ⁻¹	(nm)	(nm)	(nm)	(nm)	(nm)	(nm)
10	67	0.5	65	0.5	70	2
50	64	1	65	0.5	65	1
100	66	1	76	1	85	1
150	110	4	254	8	181	7

292 **8** References

- 293 1. F. V. D. Kammer, M. Baborowski and K. Friese, *Anal Chim Acta*, 2005, **552**, 166-174.
294 DOI: DOI 10.1016/j.aca.2005.07.049.
- 295 2. M. Kosmulski, *J Colloid Interf Sci*, 2006, **298**, 730-741. DOI: DOI
296 10.1016/j.jcis.2006.01.003.
- 297 3. R. Grombe, J. Charoud-Got, H. Emteborg, T. P. J. Linsinger, J. Seghers, S. Wagner, F.
298 von der Kammer, T. Hofmann, A. Dudkiewicz, M. Llinas, C. Solans, A. Lehner and G. Allmaier,
299 *Anal Bioanal Chem*, 2014, **406**, 3895-3907. DOI: DOI 10.1007/s00216-013-7554-1.
- 300 4. S. Simovic and C. A. Prestidge, *Langmuir*, 2003, **19**, 8364-8370. DOI: Doi
301 10.1021/La0347197.
302
303